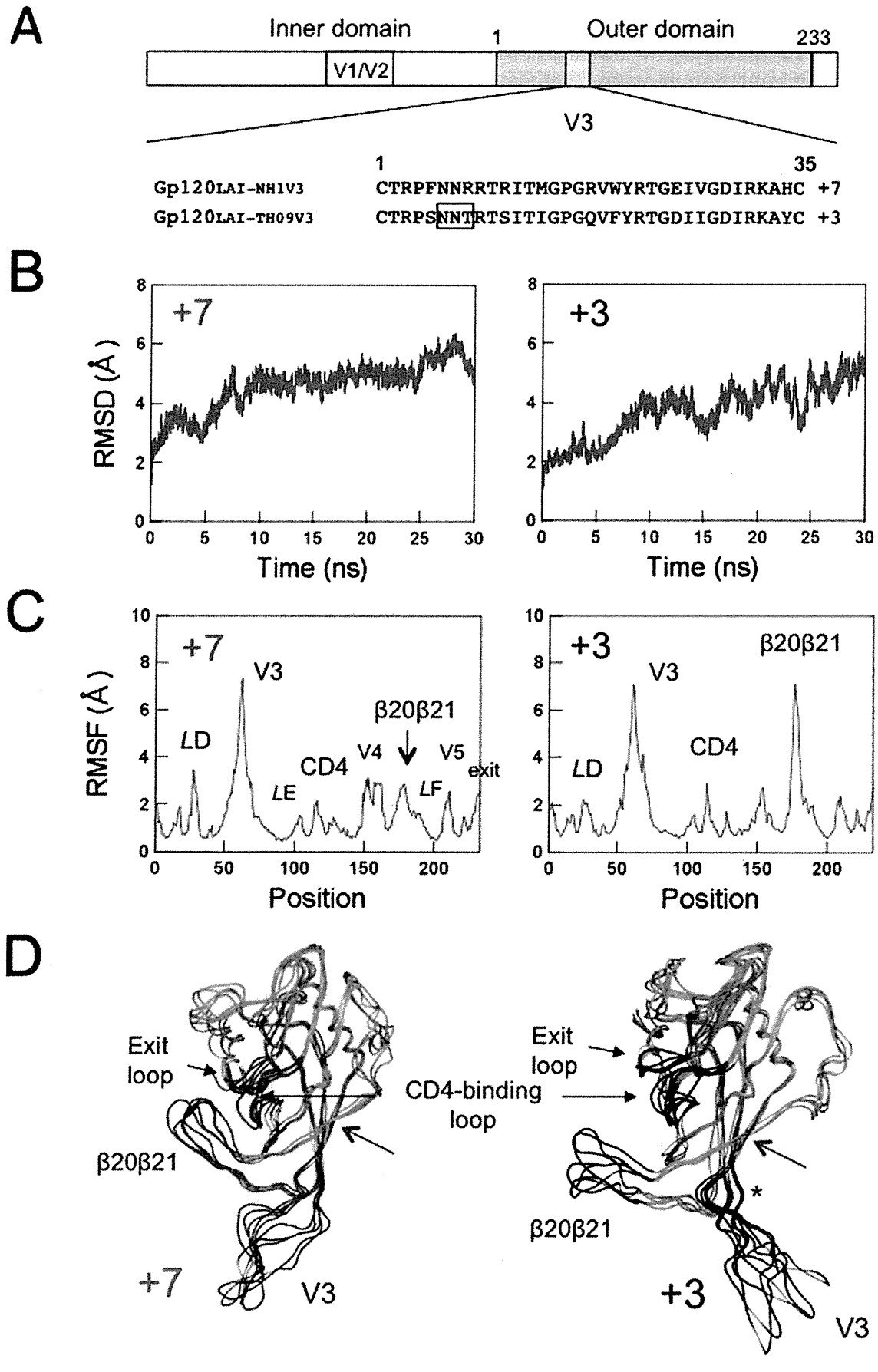
A
Inner domain
1
Outer domain
233
V1/V2
V3
1
35
Gp120LAI-NH1V3 CTRPFNNRRTRITMGPGRVWYRTGEIVGDIRKAHC +7
Gp120LAI-TH09V3 CTRPSNNTRTSITIGPGQVFYRTGDIIGDIRKAYC +3
B
+7
+3
RMSD (Å)
Time (ns)
C
+7
+3
V3
β20β21
LD
CD4
V4
V5
exit
LE
LF
RMSF (Å)
Position
D
Exit loop
CD4-binding loop
β20β21
+7
+3
V3
*

Figure 1. MD simulation of the identical gp120 outer domain carrying a V3 loop with net charge of +7 or +3. (A) Schematic representation of the gp120 open reading frame along with the amino acid sequences. The net charge indicates the number of positively charged amino acids (R, K, and H) minus the number of negatively charged amino acids (D and E) in the V3 loop. A light blue box indicates the outer domain used for the MD simulations. A pink box indicates the V3 loop. The numbers indicate amino acid positions at the outer domain (amino acids 1 to 233 in Figure 1A correspond to amino acids 256 to 489 in the gp120 of HIV-1_{LAI}) or the V3 loop. An open black box in the V3 loop sequence indicates a potential site for the N-linked glycosylation. (B–D) Left panels: $Gp120_{LAI\text{-}NH1V3}$; Right panels: $Gp120_{LAI\text{-}TH09V3}$. +7 and +3 indicate the net charges of V3 loops of the recombinant proteins. (B) Time course of RMSD during MD simulations. The RMSD values indicate the structural fluctuations of the outer domain in aqueous solution. The numbers in the horizontal axes indicate the time of MD simulation. (C) Distribution of RMSF in the gp120 outer domain. The RMSF values indicate the atomic fluctuations of the main chains of individual amino acids during 10–30 ns of MD simulations. The numbers in the horizontal axes indicate amino acid positions at the outer domain. (D) Superimposition of Gp120 models at 10, 15, 20, 25, and 30 ns of MD simulation. A green asterisk indicates approximate position of a potential N-glycosylation site at the V3 stem. A green arrow indicates the site of the disulfide bond at the V3 base.
doi:10.1371/journal.pone.0037530.g001

previous [12,13,14,15,16] neutralization studies raised the possibility that the gp120 surface might be less heterogeneous in gp120 subpopulations that have a less positively charged V3 loop, due to greater magnitudes of resistance to the antibody neutralization. To address this possibility, we performed an information entropy study using sequences in the public database. We extracted full-length gp120 amino acid sequences of HIV-1 subtype CRF01_AE that has the same evolutionary origin and is spread throughout southeast Asia [42]), and divided them into subgroups on the basis of the net charge of V3 loop (+2, +3, +4, +5, +6, +7, and +8). The sequences were used to calculate the Shannon entropy scores, *H(i)* [1], to denote the diversity of individual amino acids within each subpopulation.

Figure 3 shows the 3-D distribution of the *H(i)* scores of individual amino acids plotted on the HIV-1 gp120 crystal structure (PDB code: 2B4C [1]), where the green to orange regions were suggested to have more variable amino acids than the blue ones. In the gp120 subpopulation that has +7 V3 loop, the *H(i)* scores often exceeded 2.0 bits at many residues, reaching close to the maximum value of 4.4, i.e., the diversity was maximal, at the V5 region (Fig. 3A, left panel). Regions with high *H(i)* scores included the functional sites, such as the V3 loop and the regions around the CD4 binding site. In marked contrast, in the gp120 subpopulation carrying the +3 V3 loop, the *H(i)* scores were almost zero, i.e., the diversity was minimal, at many amino acids, but not at those in the V4, V5, and *LE* regions (Fig. 3A, right panel). Importantly, relatively high levels of conservation were also detected with amino acids in the otherwise highly variable V3 loop. Moreover, a region adjacent to the CD4 binding loop was also less heterogeneous compared with those of the gp120 subpopulation carrying +7 V3 loop (Figs. 3B). In the gp120 subpopulations carrying the +2, +3, 4, and +5 V3 loops, the *H(i)* scores were indistinguishable from each other: they were less heterogeneous than the subpopulations carrying the +6, +7, and +8 V3 loops. Similar results were obtained with HIV-1 subtype C that represents the most predominated HIV-1 in the world (data not shown).

Discussion

The ability of HIV-1 to rapidly change its phenotype greatly complicates our efforts to eradicate this virus. Elucidation of structural principles for the phenotypic change may provide a clue to control HIV-1. In this study, by combining MD simulations with antibody neutralization experiments and diversity analysis of the viral protein sequences, we studied a structural basis for the phenotypic change of HIV-1 by V3 mutations. To address this issue, we used a V3 recombinant system; we performed a computer-assisted structural study and an infection-based neutralization assay using gp120 proteins whose amino acid sequences are identical except for V3 loop. In combination with an informatics study, we obtained evidence that the HIV-1 V3 loop acts as an electrostatic modulator that influences the global structure and diversity of the interaction surface of the gp120 outer domain.

Using MD simulation, we first examined whether the V3 net charge could affect the structural dynamics of the HIV-1 gp120 outer domain surface. Initial structures of the outer domain of the two gp120s, $Gp120_{LAI\text{-}NH1V3}$ and $Gp120_{LAI\text{-}TH09V3}$, were identical before MD simulations, because the domains were both derived from HIV-1_{LAI} strain. Remarkably, however, the two molecules with distinct V3 loop exhibited markedly distinct structural dynamics following MD simulations (Figs. 1 and 2). These data strongly suggest that the V3 net charge can act as an intrinsic modulator that influences the structural dynamics of the interaction surface of the gp120 outer domain. Such a global effect on structure by a local electrostatic change has been reported with bacteriorhodopsin [43]. In general, the long-range effects of non-electrostatic contributions are negligible, whereas those of the electrostatic contributions are not [34]. Therefore, it is reasonable that the changes in overall charge of the V3 loop element caused the global effects on the gp120 structure via alteration of the electrostatic potentials of the gp120 surface.

We next studied biological impact of the structural changes predicted by MD simulations. The MD simulations suggested that the CD4 binding loop was less exposed in the $Gp120_{LAI\text{-}NH1V3}$ than the $Gp120_{LAI\text{-}NH1V3}$ (Fig. 2). The finding predicted that reduction in V3 net charge could cause reduction in neutralization sensitivity to the anti-CD4 binding site antibodies. This possibility was assessed by neutralization assay. We used infectious HIV-1_{LAI} clones having the $Gp120_{LAI\text{-}NH1V3}$ or the $Gp120_{LAI\text{-}TH09V3}$ to assess their neutralization sensitivities to the anti-CD4 binding site MAbs. Notably, we indeed observed marked reduction in the neutralization sensitivity in HIV-1_{LAI} having $Gp120_{LAI\text{-}TH09V3}$ (Table 1). The results are consistent with the structural changes predicted by MD simulations, as well as previous findings on neutralization sensitivity of HIV-1s to soluble CD4 [14,15,16].

We further studied evolutionary impact predicted by MD simulations and the neutralization studies. These studies predicted that reduction in V3 net charge could cause reduction in sequence diversity around the CD4 binding site due to reduced sensitivity to positive selection pressures of antibodies. Notably, we indeed observed marked reduction in the gp120 diversity: our Shannon entropy data show that otherwise variable surfaces of gp120, such as V3 and a region around the CD4 binding loop, are less heterogeneous in the gp120 subgroups carrying a V3 loop with a +3 charge (Fig. 3).

Previous cryo-electron microscopy studies have indicated that gp120 forms a trimer on an HIV-1 virion, where the CD4 binding sites are exposed on the outside surface in the solution [44,45,46]. Therefore, it is reasonable that gp120 with +3 V3 with less exposed CD4 binding loop is less sensitive to neutralization by anti-CD4 binding site antibodies (Table 1) and less heterogeneous around the CD4 binding site (Fig. 3). Collectively, our results

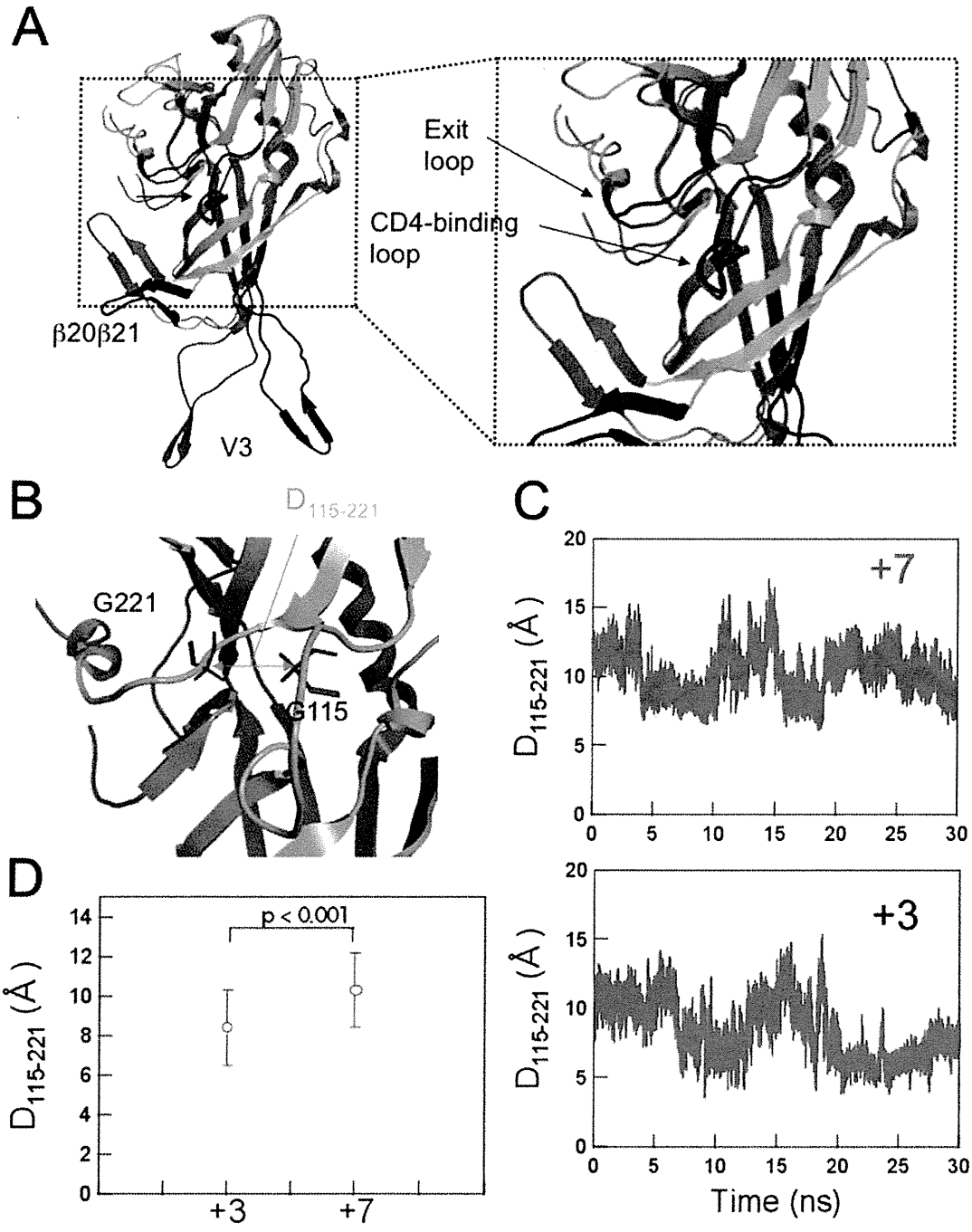

Figure 2. Comparison of the averaged 3-D models during MD simulation. (A) Superposition of the averaged structures obtained with the 40,000 snapshots obtained from 10–30 ns of MD simulations using ptraj module in Amber 9. Red and Blue ribbons: loops of $Gp120_{LAI\text{-}NH1V3}$ and $Gp120_{LAI\text{-}TH09V3}$ with V3 net charges of +7 and +3, respectively. (B–D) Configuration and structural dynamics of the CD4 binding loop. The distance between the Cα of Gly115 and the Cα of Gly221 in the CD4 binding loop was calculated to monitor configurational changes (B). The distance was monitored during the 10–30 ns of MD simulation (C) and the average distance with variance was plotted (D). +7: $Gp120_{LAI\text{-}NH1V3}$; +3: $Gp120_{LAI\text{-}TH09V3}$.
doi:10.1371/journal.pone.0037530.g002

obtained with all three approaches agree with each other and suggest that V3 net charge is an intrinsic factor that influences structural property, antibody sensitivity, and sequence diversity of CD4 binding site.

The HIV-1 gp120 outer domain has several functional or immunogenic loops involved in binding to CD4, coreceptor and antibodies. Our MD simulations predicted that V3 net charge influences fluctuation and conformation of these loops (Figs. 1 and 2). The V3-based structural modulation of the gp120 surface loops may be an effective mechanism to alter effectively the phenotype and relative fitness of HIV-1. For example, a change in the V3 net charge by mutations may induce changes in V3 conformation (Figs. 1D and 2A) [13], which in turn may influence intra- or inter-molecular interactions among gp120 monomers and thus global structure of gp120 trimer on a virion. Generation of a swarm of structural variants by V3 mutations could help generating the best-

Table 1. Neutralization sensitivity of the isogenic V3 recombinant HIV-1 to anti-gp120 monoclonal antibodies.

Antibody ID	Ig subtype	Epitopes on Gp120	ND_{50} (μg/ml)@	
			$HIV\text{-}1_{LAI\text{-}NH1V3}$	$HIV\text{-}1_{LAI\text{-}TH09V3}$
49G2	human IgG1	CD4 binding site#	0.224	>10
42F9	human IgG1	CD4 binding site#	0.934	>10
0.5δ [59]	human IgG1	CD4 binding site#	0.444	>10
4C11 [59]	human IgG2	CD4 induced structure$	>20	>10
4301	mouse IgG	broadly reactive*	0.59	0.57
8D11	human IgG1	none	>20	>10

#Neutralization epitope in the Gp120 outer domain before CD4 binding.
$Neutralization epitope induced in Gp120 after CD4 binding.
*Epitopes outside of the CD4 binding site [37].
@The effect of each antibody on viral infectivity was tested in duplicate.
doi:10.1371/journal.pone.0037530.t001

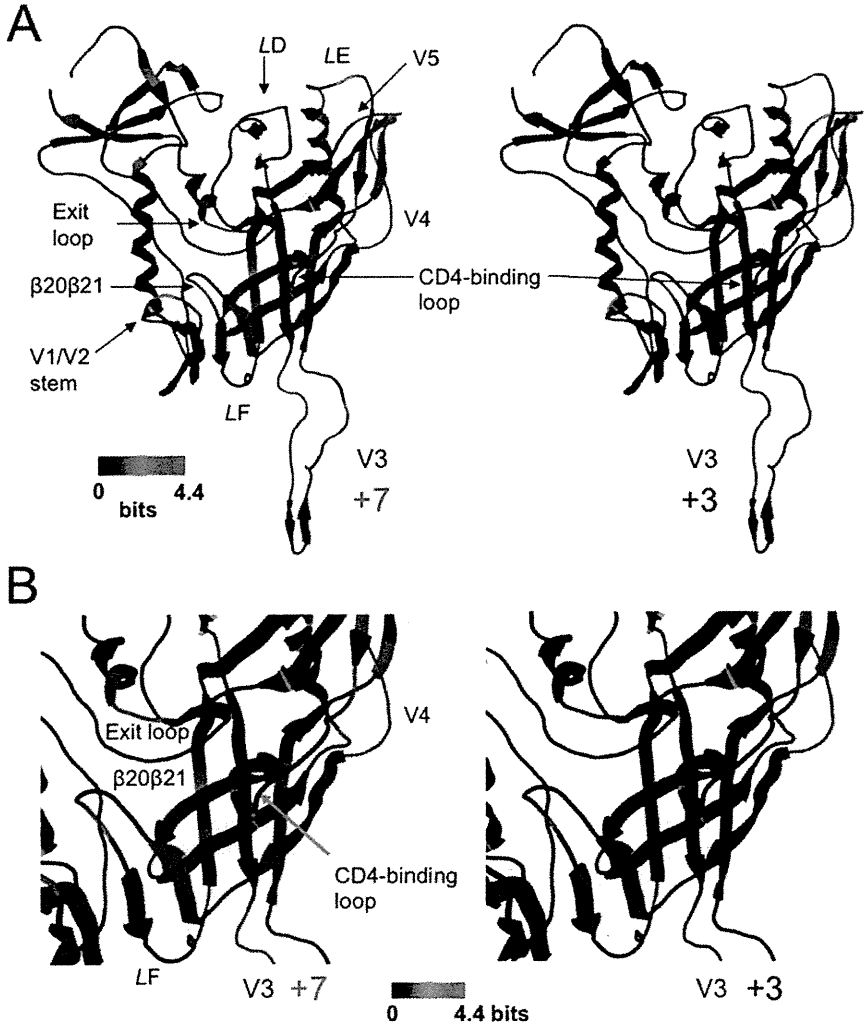

Figure 3. Diversity of the gp120 subpopulations carrying a V3 loop with net charge of +7 or +3. Full-length gp120 sequences of the HIV-1 CRF01_AE [42] were extracted from a public database, and divided into subgroups on the basis of the net charge of the V3 loop (+2~+8). The divided sequences were used to calculate the Shannon entropy, *H(i)* [63], within each subpopulation, and the *H(i)* values were plotted on the 3-D structure of gp120 (PDB code: 2B4C [1]). The results for the gp120 subgroups that have V3 loops with +7 (left panel) and +3 (right panel) charges are shown as representative. The numbers of sequences used to calculate the *H(i)* were 9 and 81 for +7 and +3, respectively. (A) Distribution of *H(i)* in the gp120 monomer. (B) Distribution of *H(i)* around the CD4 binding site.
doi:10.1371/journal.pone.0037530.g003

fit variants under changing environments during persistent infection of HIV-1 *in vivo*. Further study is necessary to address above issue.

Thus far fine structures of neither the intact gp120 monomer nor trimer are available. However, recent crystal structure study disclosed a structure of V1/V2 domain [47], which had been the major gp120 region lacking structural information. The V1/V2 domain is located on the outer surface of gp120, as is V3, and can participate in phenotypic changes of HIV-1 [48,49]. In this regard, Kwon et al [50] have found an intriguing role of gp120 variable loops; gp120 core has an intrinsic preference to form the CD4-bound conformation, whereas the variable loops, such as V1/V2 and V3 loops, play key roles in preventing conformational transitions into the CD4-bound state that is sensitive to neutralization. Thus it is conceivable that configurational changes of V3 loop by V3 mutations play roles in modulating structural dynamics of the unliganded gp120 core and neutralization sensitivity of HIV-1. Availability of the V1/V2 loop structure will promote structural study of the whole gp120 monomer containing V3 loop, V1/V2 domain, and glycans. Our findings will provide a structural basis to elucidate intra-molecular interactions of these elements, which in turn will allow the study of structure, function, and evolution of gp120 trimer. Incorporation of MD simulation into these studies will help understanding structural dynamics with which HIV-1 adjusts its relative replication fitness in nature.

Materials and Methods

Characteristics of the gp120 proteins and HIV-1s used

We used two isogenic recombinant gp120 proteins, termed $Gp120_{LAI\text{-}NH1V3}$ and $Gp120_{LAI\text{-}TH09V3}$ [35], for the present structural and neutralization studies. They differ only in their V3 loops. The $Gp120_{LAI\text{-}NH1V3}$ and $Gp120_{LAI\text{-}TH09V3}$ have the 35-amino-acid-length V3 loops from HIV-1-infected individuals in the gp120 backbone of the $HIV\text{-}1_{LAI}$ strain [35]. The net charges of the V3 loops are +7 and +3 for the $Gp120_{LAI\text{-}NH1V3}$ and $Gp120_{LAI\text{-}TH09V3}$, respectively (the V3 net charge represents the number of positively charged amino acids (R, K, and H) minus the number of negatively charged amino acids (D and E) in the V3 loop). The $HIV\text{-}1_{LAI}$ carrying the $Gp120_{LAI\text{-}NH1V3}$ ($HIV\text{-}1_{LAI\text{-}NH1V3}$) is the CXCR4 tropic virus, whereas that carrying the $Gp120_{LAI\text{-}TH09V3}$ ($HIV\text{-}1_{LAI\text{-}TH09V3}$) is the CCR5 monotropic virus [35]. The $HIV\text{-}1_{LAI\text{-}NH1V3}$ is sensitive to neutralization by antibodies with the ability to bind to the peptides containing the autologous V3 tip sequences, whereas $HIV\text{-}1_{LAI\text{-}TH09V3}$ is highly resistant to antibodies targeting the autologous V3 tip sequences [13].

MD simulation

As the initial structures for the MD simulation, we first constructed three-dimensional (3-D) models of the outer domains of the $Gp120_{LAI\text{-}NH1V3}$ and $Gp120_{LAI\text{-}TH09V3}$ by the comparative (homology) modeling method (reviewed in [33,51,52]), as described previously [13]. We used the crystal structure of HIV-1 gp120 containing an entire V3 region at a resolution of 3.30 Å (PDB code: 2B4C [1]) as the modeling template. The gp120 core is in complex with the CD4 receptor and the CD4 induced structure (CD4i) antibody X5 [1]: it represents the structure after the CD4 binding. We deleted the structures of the CD4 receptor and the X5 antibody from the 2B4C complex structure to construct the free gp120 outer domain models of $HIV\text{-}1_{LAI}$ V3 recombinant viruses by homology modeling. Then the models were subjected to the MD simulations to analyze structure and dynamics of the gp120 outer domain in the absence of the CD4 receptor and the X5 antibody interactions. The homology modeling was performed using tools available in the Molecular Operating Environment (MOE) program (MOE 2008.10; Chemical Computing Group Inc., Montreal, Quebec, Canada). The 186 amino-terminal and 27 carboxyl-terminal residues were deleted to construct the gp120 outer domain structure. We optimized the 3-D structure thermodynamically via energy minimization using an MOE and an AMBER99 force field [53]. We further refined the physically unacceptable local structure of the models based on a Ramachandran plot evaluation using MOE. MD simulations were performed as described previously [13] using the Sander module in the Amber 9 program package [54] and the AMBER99SB force field [55] with the TIP3P water model [56]. Bond lengths involving hydrogen were constrained with the SHAKE algorithm [57], and the time step for all MD simulations was set to 2 fs. A nonbonded cutoff of 12 Å was used. After heating calculations for 20 ps to 310 K using the NVT ensemble, the simulations were executed using the NPT ensemble at 1 atm at 310 K for 30 ns. Superimpositions of the $Gp120_{LAI\text{-}NH1V3}$ and $Gp120_{LAI\text{-}TH09V3}$ structures were done by coordinating atoms of amino acids along the β-sheet at the gp120 outer domain. We performed two independent MD simulations with distinct MD codes and obtained similar results. Therefore, we present here the data set from one of the MD simulations as a representation.

Calculation of the root mean square deviation (RMSD) and root mean square fluctuation (RMSF)

The RMSD values between the heavy atoms of the two superposed proteins were used to measure the overall structural differences between the two proteins [34]. We also calculated the RMSF to provide information about the atomic fluctuations during MD simulations [34]. In this study, we calculated the RMSF of the main chains of individual amino acids using the 40,000 snapshots obtained from MD simulations of 10–30 ns. The average structures during the last 20 ns of MD simulations were used as reference structures for the calculation of the RMSF. Both the RMSD and RMSF were calculated using the ptraj module in Amber 9 [34].

Monoclonal antibodies (MAbs)

The 49G2, 42F9, 0.5δ and 4C11 antibodies used for the neutralization assay were the human MAbs established from an HIV-1-infected patient with long-term non-progressive illness. Human blood samples were collected after signed informed consent in accordance with study protocol and informed consent reviewed and approved by Ethics committee for clinical research & advanced medical technology at the Faculty of Life Science Kumamoto University. B cells from the patient's peripheral blood mononuclear cells were transformed by EBV, followed by cloning as described previously [58]. The culture supernatant from an individual clone was screened for the reactivity to $gp120_{SF2}$ by an enzyme-linked immunosorbent assay (ELISA). The specificity of antibodies was determined by gp120 capture ELISA and FACS analysis as described previously [59]. Briefly, reactivity of the mAbs against monomeric gp120 of $HIV\text{-}1_{SF2}$ was measured with a gp120 capture assay in the absence or presence of soluble CD4 (0.5 μg/ml). Decrease in the binding activity was observed for the mAbs 0.5δ, 49G2, and 42F9 in the presence of soluble CD4, whereas enhancement in the reactivity was detected for the mAb 4C11. Reactivity of the mAbs against envelope protein on the cell surface was measured with a FACS analysis of PM1 cells chronically infected with JR-FL in the absence or presence of soluble CD4 (0.5 μg/ml). No significant difference was observed for the binding profiles of 0.5δ, 49G2, and 42F9 in the presence of

soluble CD4, whereas marked enhancement of binding was observed for the 4C11 in the presence of soluble CD4. Based on these binding data, we classified 49G2, 42F9, and 0.5δ as CD4 binding site Mabs, and 4C11 as a CD4-induced epitope. All MAbs used in this study were purified by affinity chromatography on Protein A Sepharose. A human MAb 8D11 was used as a negative control for the neutralization assay. Mouse MAb 4301 was purchased from Advanced BioScience Laboratories, Inc. (Kensington, MD). The 4301 was raised with a mixture of purified gp120 of HIV-1_{IIIB} and HIV-1_{MN} and broadly reactive with the gp120 of different HIV-1 isolates [37].

Neutralization assay

We used the two above-described V3 recombinant HIV-1s, HIV-$1_{LAI\text{-}NH1V3}$ and HIV-$1_{LAI\text{-}TH09V3}$ [35], for the neutralization study. The HIV-1 cell-free viruses were prepared by transfection of the plasmid DNAs into HeLa cells as described previously [24,35,60]. The neutralization activities of antibodies were measured in a single-round viral infectivity assay using $CD4^+CXCR4^+CCR5^+$ HeLa cells [36] as described previously [13]. Briefly, equal infectious titers of viruses (300 blue-cell-forming units) were incubated with serially diluted MAb preparations (0.03–10 μg/ml) for 1 hour at 37°C. The cells were infected with the virus-antibody mixture for 48 hours at 37°C, fixed, and stained with 5-bromo-4-chloro-3-indolyl-β-D-galactopyranoside. Each antibody dilution was tested in duplicate, and the means of the positive blue cell numbers were used to calculate the 50% inhibition dose of viral infectivity (ND_{50}).

Analysis of amino acid diversity

Amino acid diversity at individual sites of the HIV-1 gp120 sequences was analyzed with Shannon entropy scores as described previously [13,61,62]. Full-length gp120 amino acid sequences of the HIV-1 subtypes CRF01_AE and C were obtained from the HIV Sequence Database (http://www.hiv.lanl.gov/content/sequence/HIV/mainpage.html). The sequences were divided into subgroups based on the net charge of V3 loop (+2~+8) using a software system, InforSense 5.0.1 (InforSense Ltd. http://www.inforsense.com/); arginine (R), lysine (K), and histidine (H) were counted as +1, aspartic acid (D) and glutamic acid (E) as -1, and other amino acids as 0. The numbers of sequences used for the analysis of CRF01_AE were 11, 81, 57, 28, 18, 9, and 4 for +2, +3, +4, +5, +6, +7, and +8, respectively. The amino acid diversity within each V3 subpopulation of the same HIV-1 subtype was calculated using Shannon's formula [63]:

$$H(i) = -\sum_{x_i} p(x_i)\log_2 p(x_i) \quad \{x_i = \text{G, A, I, V, ...}\},$$

where $H(i)$, $p(x_i)$, and i indicate the amino acid entropy score of a given position, the probability of occurrence of a given amino acid at the position, and the number of the position, respectively. An $H(i)$ score of zero indicates absolute conservation, whereas 4.4 bits indicates complete randomness. The $H(i)$ scores were displayed on the 3-D structure of an HIV-1 gp120 (PDB code: 2B4C [1]).

Acknowledgments

We thank Shingo Kiyoura (SGI Japan, Ltd.), and Kaori Sawada and Takashi Ikegami (Ryoka Systems Inc.) for their support with the computational analysis. We thank Hirotaka Ode of the Pathogen Genomics Center for his helpful comments on the manuscript.

Author Contributions

Conceived and designed the experiments: MY SN HS. Performed the experiments: MY SN HS. Analyzed the data: MY SN HS. Contributed reagents/materials/analysis tools: KY SM. Wrote the paper: MY HS.

References

1. Huang CC, Tang M, Zhang MY, Majeed S, Montabana E, et al. (2005) Structure of a V3-containing HIV-1 gp120 core. Science 310: 1025–1028.
2. Huang CC, Lam SN, Acharya P, Tang M, Xiang SH, et al. (2007) Structures of the CCR5 N terminus and of a tyrosine-sulfated antibody with HIV-1 gp120 and CD4. Science 317: 1930–1934.
3. Choe H, Farzan M, Sun Y, Sullivan N, Rollins B, et al. (1996) The beta-chemokine receptors CCR3 and CCR5 facilitate infection by primary HIV-1 isolates. Cell 85: 1135–1148.
4. Speck RF, Wehrly K, Platt EJ, Atchison RE, Charo IF, et al. (1997) Selective employment of chemokine receptors as human immunodeficiency virus type 1 coreceptors determined by individual amino acids within the envelope V3 loop. J Virol 71: 7136–7139.
5. Xiao L, Owen SM, Goldman I, Lal AA, deJong JJ, et al. (1998) CCR5 coreceptor usage of non-syncytium-inducing primary HIV-1 is independent of phylogenetically distinct global HIV-1 isolates: delineation of consensus motif in the V3 domain that predicts CCR-5 usage. Virology 240: 83–92.
6. Cho MW, Lee MK, Carney MC, Berson JF, Doms RW, et al. (1998) Identification of determinants on a dualtropic human immunodeficiency virus type 1 envelope glycoprotein that confer usage of CXCR4. J Virol 72: 2509–2515.
7. Goudsmit J, Debouck C, Meloen RH, Smit L, Bakker M, et al. (1988) Human immunodeficiency virus type 1 neutralization epitope with conserved architecture elicits early type-specific antibodies in experimentally infected chimpanzees. Proc Natl Acad Sci U S A 85: 4478–4482.
8. Rusche JR, Javaherian K, McDanal C, Petro J, Lynn DL, et al. (1988) Antibodies that inhibit fusion of human immunodeficiency virus-infected cells bind a 24-amino acid sequence of the viral envelope, gp120. Proc Natl Acad Sci U S A 85: 3198–3202.
9. Javaherian K, Langlois AJ, McDanal C, Ross KL, Eckler LI, et al. (1989) Principal neutralizing domain of the human immunodeficiency virus type 1 envelope protein. Proc Natl Acad Sci U S A 86: 6768–6772.
10. Cavacini LA, Duval M, Robinson J, Posner MR (2002) Interactions of human antibodies, epitope exposure, antibody binding and neutralization of primary isolate HIV-1 virions. Aids 16: 2409–2417.
11. Lusso P, Earl PL, Sironi F, Santoro F, Ripamonti C, et al. (2005) Cryptic nature of a conserved, CD4-inducible V3 loop neutralization epitope in the native envelope glycoprotein oligomer of CCR5-restricted, but not CXCR4-using, primary human immunodeficiency virus type 1 strains. J Virol 79: 6957–6968.
12. Bou-Habib DC, Roderiquez G, Oravecz T, Berman PW, Lusso P, et al. (1994) Cryptic nature of envelope V3 region epitopes protects primary monocytotropic human immunodeficiency virus type 1 from antibody neutralization. J Virol 68: 6006–6013.
13. Naganawa S, Yokoyama M, Shiino T, Suzuki T, Ishigatsubo Y, et al. (2008) Net positive charge of HIV-1 CRF01_AE V3 sequence regulates viral sensitivity to humoral immunity. PLoS One 3: e3206.
14. Hwang SS, Boyle TJ, Lyerly HK, Cullen BR (1992) Identification of envelope V3 loop as the major determinant of CD4 neutralization sensitivity of HIV-1. Science 257: 535–537.
15. Willey RL, Theodore TS, Martin MA (1994) Amino acid substitutions in the human immunodeficiency virus type 1 gp120 V3 loop that change viral tropism also alter physical and functional properties of the virion envelope. J Virol 68: 4409–4419.
16. Willey RL, Martin MA, Peden KW (1994) Increase in soluble CD4 binding to and CD4-induced dissociation of gp120 from virions correlates with infectivity of human immunodeficiency virus type 1. J Virol 68: 1029–1039.
17. Kwong PD, Wyatt R, Robinson J, Sweet RW, Sodroski J, et al. (1998) Structure of an HIV gp120 envelope glycoprotein in complex with the CD4 receptor and a neutralizing human antibody. Nature 393: 648–659.
18. Fouchier RA, Groenink M, Kootstra NA, Tersmette M, Huisman HG, et al. (1992) Phenotype-associated sequence variation in the third variable domain of the human immunodeficiency virus type 1 gp120 molecule. J Virol 66: 3183–3187.
19. Chesebro B, Wehrly K, Nishio J, Perryman S (1992) Macrophage-tropic human immunodeficiency virus isolates from different patients exhibit unusual V3 envelope sequence homogeneity in comparison with T-cell-tropic isolates: definition of critical amino acids involved in cell tropism. J Virol 66: 6547–6554.
20. Milich L, Margolin B, Swanstrom R (1993) V3 loop of the human immunodeficiency virus type 1 Env protein: interpreting sequence variability. J Virol 67: 5623–5634.
21. Milich L, Margolin BH, Swanstrom R (1997) Patterns of amino acid variability in NSI-like and SI-like V3 sequences and a linked change in the CD4-binding domain of the HIV-1 Env protein. Virology 239: 108–118.

22. de Jong J-J, de Ronde A, Keulen W, Tersmette M, Goudsmit J (1992) Minimal requirements for the human immunodeficiency virus type 1 V3 domain to support the syncytium-inducing phenotype: analysis by single amino acid substitution. J Virol 66: 6777–6780.
23. Shioda T, Oka S, Ida S, Nokihara K, Toriyoshi H, et al. (1994) A naturally occurring single basic amino acid substitution in the V3 region of the human immunodeficiency virus type 1 env protein alters the cellular host range and antigenic structure of the virus. J Virol 68: 7689–7696.
24. Kato K, Sato H, Takebe Y (1999) Role of naturally occurring basic amino acid substitutions in the human immunodeficiency virus type 1 subtype E envelope V3 loop on viral coreceptor usage and cell tropism. J Virol 73: 5520–5526.
25. Thorpe IF, Brooks CL, 3rd (2007) Molecular evolution of affinity and flexibility in the immune system. Proc Natl Acad Sci U S A 104: 8821–8826.
26. Lu HP, Xun L, Xie XS (1998) Single-molecule enzymatic dynamics. Science 282: 1877–1882.
27. Astumian RD (1997) Thermodynamics and kinetics of a Brownian motor. Science 276: 917–922.
28. Garcia-Viloca M, Gao J, Karplus M, Truhlar DG (2004) How enzymes work: analysis by modern rate theory and computer simulations. Science 303: 186–195.
29. Karplus M, Kuriyan J (2005) Molecular dynamics and protein function. Proc Natl Acad Sci U S A 102: 6679–6685.
30. Dodson GG, Lane DP, Verma CS (2008) Molecular simulations of protein dynamics: new windows on mechanisms in biology. EMBO Rep 9: 144–150.
31. Miyamoto T, Yokoyama M, Kono K, Shioda T, Sato H, et al. (2011) A single amino acid of human immunodeficiency virus type 2 capsid protein affects conformation of two external loops and viral sensitivity to TRIM5alpha. PLoS One 6: e22779.
32. Ode H, Yokoyama M, Kanda T, Sato H (2011) Identification of folding preferences of cleavage junctions of HIV-1 precursor proteins for regulation of cleavability. J Mol Model 17: 391–399.
33. Baker D, Sali A (2001) Protein structure prediction and structural genomics. Science 294: 93–96.
34. Case DA, Cheatham TE, 3rd, Darden T, Gohlke H, Luo R, et al. (2005) The Amber biomolecular simulation programs. J Comput Chem 26: 1668–1688.
35. Sato H, Kato K, Takebe Y (1999) Functional complementation of the envelope hypervariable V3 loop of human immunodeficiency virus type 1 subtype B by the subtype E V3 loop. Virology 257: 491–501.
36. Hachiya A, Aizawa-Matsuoka S, Tanaka M, Takahashi Y, Ida S, et al. (2001) Rapid and simple phenotypic assay for drug susceptibility of human immunodeficiency virus type 1 using CCR5-expressing HeLa/CD4(+) cell clone 1–10 (MAGIC-5). Antimicrob Agents Chemother 45: 495–501.
37. di Marzo Veronese F, Rahman R, Pal R, Boyer C, Romano J, et al. (1992) Delineation of immunoreactive, conserved regions in the external glycoprotein of the human immunodeficiency virus type 1. AIDS Res Hum Retroviruses 8: 1125–1132.
38. Simmonds P, Balfe P, Ludlam CA, Bishop JO, Brown AJ (1990) Analysis of sequence diversity in hypervariable regions of the external glycoprotein of human immunodeficiency virus type 1. J Virol 64: 5840–5850.
39. Burns DP, Desrosiers RC (1994) Envelope sequence variation, neutralizing antibodies, and primate lentivirus persistence. Curr Top Microbiol Immunol 188: 185–219.
40. Bonhoeffer S, Holmes SE, Nowak M (1995) Causes of HIV diversity. Nature 376: 125.
41. Lukashov VV, Kuiken CL, Goudsmit J (1995) Intrahost human immunodeficiency virus type 1 evolution is related to length of the immunocompetent period. J Virol 69: 6911–6916.
42. Buonaguro L, Tornesello ML, Buonaguro FM (2007) Human immunodeficiency virus type 1 subtype distribution in the worldwide epidemic: pathogenetic and therapeutic implications. J Virol 81: 10209–10219.
43. Brown LS, Kamikubo H, Zimanyi L, Kataoka M, Tokunaga F, et al. (1997) A local electrostatic change is the cause of the large-scale protein conformation shift in bacteriorhodopsin. Proc Natl Acad Sci U S A 94: 5040–5044.
44. Wu SR, Loving R, Lindqvist B, Hebert H, Koeck PJ, et al. (2010) Single-particle cryoelectron microscopy analysis reveals the HIV-1 spike as a tripod structure. Proc Natl Acad Sci U S A 107: 18844–18849.
45. White TA, Bartesaghi A, Borgnia MJ, Meyerson JR, de la Cruz MJ, et al. (2010) Molecular architectures of trimeric SIV and HIV-1 envelope glycoproteins on intact viruses: strain-dependent variation in quaternary structure. PLoS Pathog 6: e1001249.
46. Hu G, Liu J, Taylor KA, Roux KH (2011) Structural comparison of HIV-1 envelope spikes with and without the V1/V2 loop. J Virol 85: 2741–2750.
47. McLellan JS, Pancera M, Carrico C, Gorman J, Julien JP, et al. (2012) Structure of HIV-1 gp120 V1/V2 domain with broadly neutralizing antibody PG9. Nature 480: 336–343.
48. Shibata J, Yoshimura K, Honda A, Koito A, Murakami T, et al. (2007) Impact of V2 mutations on escape from a potent neutralizing anti-V3 monoclonal antibody during in vitro selection of a primary human immunodeficiency virus type 1 isolate. J Virol 81: 3757–3768.
49. Ogert RA, Lee MK, Ross W, Buckler-White A, Martin MA, et al. (2001) N-linked glycosylation sites adjacent to and within the V1/V2 and the V3 loops of dualtropic human immunodeficiency virus type 1 isolate DH12 gp120 affect coreceptor usage and cellular tropism. J Virol 75: 5998–6006.
50. Kwon YD, Finzi A, Wu X, Dogo-Isonagie C, Lee LK, et al. (2012) Unliganded HIV-1 gp120 core structures assume the CD4-bound conformation with regulation by quaternary interactions and variable loops. Proc Natl Acad Sci U S A 109: 5663–5668.
51. Sanchez R, Pieper U, Melo F, Eswar N, Marti-Renom MA, et al. (2000) Protein structure modeling for structural genomics. Nat Struct Biol 7 Suppl: 986–990.
52. Marti-Renom MA, Stuart AC, Fiser A, Sanchez R, Melo F, et al. (2000) Comparative protein structure modeling of genes and genomes. Annu Rev Biophys Biomol Struct 29: 291–325.
53. Ponder JW, Case DA (2003) Force fields for protein simulations. Adv Protein Chem 66: 27–85.
54. Case DA, Darden TA, Cheatham TE, Simmerling CL, Wang J, et al. (2006) AMBER 9. University of California: San Francisco.
55. Hornak V, Abel R, Okur A, Strockbine B, Roitberg A, et al. (2006) Comparison of multiple Amber force fields and development of improved protein backbone parameters. Proteins 65: 712–725.
56. Jorgensen WL, Chandrasekhar J, Madura JD, Impey RW, Klein ML (1983) Comparison of simple potential functions for simulating liquid water. J Chem Phys 79: 926–935.
57. Ryckaert JP, Ciccotti G, Berendsen HJC (1977) Numerical integration of the Cartesian equations of motion of a system with constraints: Molecular dynamics of n-alkanes. J Comput Phys 23: 327–341.
58. Matsushita S, Robert-Guroff M, Rusche J, Koito A, Hattori T, et al. (1988) Characterization of a human immunodeficiency virus neutralizing monoclonal antibody and mapping of the neutralizing epitope. J Virol 62: 2107–2114.
59. Yoshimura K, Harada S, Shibata J, Hatada M, Yamada Y, et al. (2010) Enhanced Exposure of Human Immunodeficiency Virus Type 1 Primary Isolate Neutralization Epitopes through Binding of CD4 Mimetic Compounds. J Virol.
60. Shiino T, Kato K, Kodaka N, Miyakuni T, Takebe Y, et al. (2000) A group of V3 sequences from human immunodeficiency virus type 1 subtype E non-syncytium-inducing, CCR5-using variants are resistant to positive selection pressure. J Virol 74: 1069–1078.
61. Motomura K, Oka T, Yokoyama M, Nakamura H, Mori H, et al. (2008) Identification of monomorphic and divergent haplotypes in the 2006–2007 norovirus GII/4 epidemic population by genomewide tracing of evolutionary history. J Virol 82: 11247–11262.
62. Oka T, Yokoyama M, Katayama K, Tsunemitsu H, Yamamoto M, et al. (2009) Structural and biological constraints on diversity of regions immediately upstream of cleavage sites in calicivirus precursor proteins. Virology 394: 119–129.
63. Shannon CE (1997) The mathematical theory of communication. 1963. MD Comput 14: 306–317.

NIH Public Access
Author Manuscript
Cell Mol Biol (Noisy-le-grand). Author manuscript: available in PMC 2013 March 30.

Published in final edited form as:
Cell Mol Biol (Noisy-le-grand). ; 58(1): 71–79.

Preparation of Biologically Active Single-Chain Variable Antibody Fragments that Target the HIV-1 gp120 V3 Loop

Y.T. Ong[1,2], **K.A. Kirby**[1,2], **A. Hachiya**[1,2,3], **L.A. Chiang**[1,2], **B. Marchand**[1,2], **K. Yoshimura**[4], **T. Murakami**[5], **K. Singh**[1,2], **S. Matsushita**[4], and **S.G. Sarafianos**[1,2,6,✉]

[1]Christopher S. Bond Life Sciences Center, University of Missouri School of Medicine, Columbia, MO 65211, USA

[2]Department of Molecular Microbiology & Immunology, University of Missouri School of Medicine, Columbia, MO 65211, USA

[3]AIDS Clinical Center, National Center for Global Health and Medicine, Tokyo 162-8655, Japan

[4]Division of Clinical Retrovirology and Infectious Diseases, Center for AIDS Research, Kumamoto University, 2-2-1 Honjo, Kumamoto 860-0811, Japan

[5]The Chemo-Sero-Therapeutic Research Institute (Kaketsuken), Kyokushi, Kikuchi, Kumamoto 869-1298, Japan

[6]Department of Biochemistry, University of Missouri, Columbia, MO 65211, USA

Abstract

KD-247 is a humanized monoclonal antibody that targets the third hypervariable (V3) loop of gp120. It can efficiently neutralize a broad panel of clade B, but not non-clade B, HIV-1 isolates. To overcome this limitation, we are seeking to prepare genetically-engineered single-chain variable fragments (scFvs) of KD-247 that will have broader neutralizing activity against both clade B and non-clade B HIV-1 isolates. Initial attempts of optimizing the expression of KD-247 scFv have resulted in the formation of insoluble protein. Therefore, we have established purification protocols to recover, purify, and refold the KD-247 scFv from inclusion bodies. The protocol involved step-wise refolding of denatured scFv by dilution, dialysis, and on-column nickel-affinity purification. Monomeric scFv was further purified by size-exclusion chromatography. Using far UV circular dichroism (CD) spectroscopy we confirmed the expected beta-sheet profile of the refolded KD-247 scFv. Importantly, the refolded KD-247 scFv showed neutralizing activity against replication-competent HIV-1 BaL and JR-FL Env pseudotyped HIV-1, at potency comparable to that of the native full-size KD-247 antibody. Ongoing studies focus on the application of this system in generating KD-247 scFv variants with the ability to neutralize clade B and non-clade B HIV-1 isolates.

Keywords

KD-247; neutralizing antibody; HIV; gp120; V3 loop; scFv; purification; refolding

✉Corresponding author: Stefan G. Sarafianos 471d Christopher S. Bond Life Sciences Center, 1201 Rollins St., Columbia, MO 65211, USA Tel: +1 (573) 882-4338 Fax: +1 (573) 884-9676 sarafianoss@missouri.edu.

NIH-PA Author Manuscript
NIH-PA Author Manuscript
NIH-PA Author Manuscript

NIH-PA Author Manuscript
NIH-PA Author Manuscript
NIH-PA Author Manuscript

INTRODUCTION

The replication life-cycle of human immunodeficiency virus type 1 (HIV-1) begins with the cell-free virus attachment to the host cell, either a CD4-positive T lymphocyte or macrophage, through the interaction of HIV-1 glycoprotein 120 (gp120) with the host CD4 receptor (6,21). Conformational changes in the HIV-1 envelope glycoprotein (Env) trimer trigger the formation of the bridging sheet and the exposure of the third hypervariable (V3) loop, which are responsible for the binding to CCR5 or CXCR-4 co-receptor on the host cell (9,24,35,36,37,38,40,47). This is followed by additional conformational changes in the gp120/gp41 complex that eventually lead to fusion of the viral envelope with the cellular membrane to allow release of the viral contents into the host cell for viral replication (10,29,44,46). HIV-1 entry is a critical step to target in order to prevent infection and block viral replication.

For more than two decades since the discovery of HIV-1, exhaustive efforts have been put into the discovery of a vaccine against this devastating human pathogen. However, HIV-1 has evolved multiple mechanisms to evade the host antibody response, making the ideal mission of finding a cure against HIV-1 extremely challenging (23,32,43). Despite the failure of developing a successful HIV-1 vaccine, Highly Active Anti-Retroviral Therapy (HAART) has proven to be a highly effective treatment regimen against HIV-1 infection (33). HAART involves the administration of a combination of at least three antiretroviral drugs to overcome the ability of HIV-1 to become resistant against a particular drug. Among the 32 FDA-approved antiretroviral drugs against HIV-1, there are only two inhibitors of viral entry. Maraviroc targets the CCR5 co-receptor, while enfuvirtide binds to gp41 and blocks the fusion event (7,11,25). Therefore, the development of novel therapeutics against HIV-1 entry is still very crucial. Neutralizing antibodies discovered through the HIV-1 vaccine studies can be potential therapeutics for prophylaxis treatment (2,31,45). Although some broadly neutralizing antibodies such as 2G12, 2F5, 4E10, b12, PG9, PG16, HJ16, VRC01, VRC03 have been reported (16), there is a very large number of neutralizing antibodies with narrow neutralization profile that still can be improved through antibody engineering.

Development and advancement in the field of antibody engineering has enabled researchers to improve the properties of an antibody of interest using techniques such as phage display (3,4,28,41). To improve the effectiveness of clade-specific neutralizing antibodies, we have applied structural and molecular modeling approaches to help us engineer second-generation antibodies based on rational structure-based design. In this study, we are interested in investigating KD-247, a humanized monoclonal antibody (mAb) currently in clinical trials that binds the conserved V3 loop of gp120 and efficiently neutralizes many clade B HIV-1 isolates, which possess V3 loop with $Glycine^{312}$-$Proline^{313}$-$Glycine^{314}$-$Arginine^{315}$ (GPGR) motif (12,27). Similar to other anti-V3 mAbs, KD-247 cannot neutralize non-clade B HIV-1 isolates, which are the predominant HIV-1 infection cases arising today. Interestingly, $Glycine^{312}$-$Proline^{313}$-$Glycine^{314}$-$Glutamine^{315}$ (GPGQ) motif is highly conserved among non-clade B HIV-1. To better understand the molecular interaction of KD-247 with its epitope, Isoleucine-Glycine-Proline-Glycine-Arginine (IGPGR) at positions 311 to 315, which is located at the tip region of HIV-1 V3 loop (12,27), we have constructed KD-247 in the form of a single-chain variable fragment (scFv).

scFvs are antibody fragments containing a single variable heavy (V_H) domain and a single variable light (V_L) domain connected by a flexible amino acid linker (4,5,13,17,18,22,28). scFvs have been widely applied in the field of antibody engineering, especially in phage display for the discovery of antibodies specific for the antigen of interest and for the affinity maturation of the existing antibodies (28,41). Expression of scFv in the periplasmic space of

NIH-PA Author Manuscript NIH-PA Author Manuscript NIH-PA Author Manuscript

Escherichia coli (*E. coli*) has been described (18,20). Alternatively, scFvs can be obtained by overexpression in the cytoplasm of *E. coli* using pET system with the caveat that they are usually expressed in inclusion bodies (14,15,26,39,42). Nonetheless, many studies have shown that the purification of scFvs from inclusion bodies is an obstacle that can be overcome through *in vitro* refolding (14,15,26,39,42). Here, we have established a system to obtain soluble, active KD-247 scFv, which we are now applying in our ongoing study to generate KD-247 variants to confirm the V3 loop binding site and to evaluate their neutralization profiles. This protocol can be useful for the successful purification of other scFvs that are expressed as inclusion bodies in bacterial systems.

MATERIALS AND METHODS

Construction of KD-247 scFv Expression Vector

The amino acid sequences of the variable domains of the heavy (V_H) and the light (V_L) chains of the KD-247 antigen binding fragment (F_{ab}) were obtained from the Protein Data Bank (PDB: 3NTC_H and 3NTC_L). The KD-247 scFv was designed in the order of the V_H sequence, a (Glycine-Glycine-Glycine-Glycine-Serine)$_4$ linker, and the V_L sequence. The gene of KD-247 scFv was optimized for protein expression in *E. coli* and synthesized by Epoch Life Science, Inc. Using *Bam HI* and *Hind III* restriction sites, the KD-247 scFv gene was subcloned into a pET28a3c plasmid, which was modified from pET28a(+) (Novagen, EMD4Biosciences) with insertion of the Rhinovirus 3C protease cleavage site downstream of a 6X Histidine tag. The ligated product was transformed in *Escherichia coli* (*E. coli*) strain DH5α. The gene sequence of the pET28a3c-KD247-scFv construct was confirmed by sequencing using T7 promoter and T7 terminator primers (Novagen, EMD4Biosciences).

Optimization of KD-247 scFv Expression in E. coli

The KD-247 scFv expression vector (pET28a3c-KD247-scFv) was transformed into *E. coli* expression strain Origami 2 (DE3) pLysS (Novagen) by heat-shock. A single colony of transformed cell was inoculated in 10 ml Luria-Bertani broth (LB) containing 50 μg/ml kanamycin, 34 μg/ml chloramphenicol, and 10 μg/ml tetracycline at 37 °C with shaking at 225 rpm for overnight. 2 ml of the overnight culture was transferred into 200 ml LB containing the antibiotics and continue shaking at 37 °C until optical density at 600 nm (OD_{600nm}) reaches mid-log phase (0.6 - 0.8). 50 ml of culture was transferred into three other sterile flasks. The remaining culture was incubated at 37 °C with shaking for three hours without addition of Isopropyl β-D-1-thiogalactopyranoside (IPTG). Cultures in the three other flasks were induced with IPTG at final concentration of 0.25 mM, 0.5 mM, and 1 mM respectively and continue shaking at 37 °C for three hours. Cells were harvested by centrifugation at 4,200 x g for 15 min at 4 °C and pellets were stored at -20 °C. The same protocol was used for growing and inducing cultures at 30 °C. To optimize scFv expression in various *E. coli* expression strains, including BL21 (DE3), Rosetta 2 (DE3) (Novagen), BL21 Gold (DE3) pLysS (Stratagene), and BL21 Star (DE3) (Invitrogen), a similar protocol is used with modifications of the growing culture (in LB with the appropriate antibiotics) at 37 °C and inducing expression with 0.5 mM IPTG.

Each frozen cell pellet was thawed on ice and resuspended in 5 ml lysis buffer containing 50 mM Tris-HCl pH 8.0, 150 mM NaCl, 1 mM EDTA, 0.1% Triton X-100, 1 mM phenylmethylsulfonyl fluoride (PMSF), and 250 μg/ml lysozyme. 10 μg/ml DNAse and 20 mM $MgSO_4$ were added to cell suspension and incubated on ice for 30 min before centrifugation at 13,000 × g for 20 min at 4 °C. Cell lysates in the supernatant were collected in new tubes. The pellets and lysates of both non-induced and induced samples were analyzed by sodium dodecyl sulfate polyacrylamide gel electrophoresis (SDS-PAGE).

NIH-PA Author Manuscript
NIH-PA Author Manuscript
NIH-PA Author Manuscript

Purification of KD-247 scFv from Inclusion Bodies

KD-247 scFv was expressed in *E. coli* BL21 (DE3) competent cells as described above with some modifications. 10 ml of overnight culture grown in the presence of kanamycin was transferred to 500 ml of LB containing kanamycin. Protein expression was induced at OD_{600nm} = 1.0 with addition of IPTG (0.5 mM) and incubation at 37 °C for three hours. Harvested cells in the pellet form were stored at -20 °C overnight. The cell pellet was resuspended in 25 ml Lysis Buffer (Table 1). The cell resuspension was then sonicated on ice with 30 seconds on-off cycle for 10 min. The cell lysate was centrifuged at 13,000 × g for 15 min at 4 °C. The pellet was first washed with 25 ml Wash Buffer A (Table 1) with gentle shaking at 4 °C overnight. After centrifugation at 13,000 × g for 15 min at 4 °C, the pellet was washed with 25 ml Wash Buffer B (Table 1) using the same procedure. The pellet containing inclusion bodies was solubilized in 10 ml Denaturing Buffer (Table 1) using the previous procedure. Finally, the denatured protein was collected from the supernatant after centrifugation and kept at 4 °C until use. Concentration of the denatured KD-247 scFv protein was estimated using a Nanodrop with the calculated extinction coefficient (62.3 × 10^3 $M^{-1}cm^{-1}$) and molecular weight (30.2 kDa).

Refolding of KD-247 scFv

The denatured KD-247 scFv protein was diluted in 100 ml Refolding Buffer A (Table 1). The diluted KD-247 scFv sample was dialyzed in Spectra/Por® Dialysis Membrane MWCO 3500 (Spectrum Laboratories, Inc.) against Refolding Buffer B (Table 1) at 4°C overnight. These refolding steps were repeated four times using the same Refolding Buffer B. Partially refolded scFv was loaded onto a 5 ml HisTrap column (GE Healthcare) using an ÄKTAprime plus FPLC system. Next, the column was washed with a gradient of Refolding Buffer B against Refolding Buffer C (Table 1). Column-bound refolded protein was eluted using a gradient of Refolding Buffer C against Elution Buffer (Table 1). Elution fractions corresponding to ~30 kDa protein were pooled and buffer exchanged against 1X phosphate-buffered saline (PBS) pH 7.6 using PD-10 desalting columns. Refolded KD-247 scFv was further separated by gel filtration on a HiPrep 26/60 Sephacryl S200 HR column (GE Healthcare) equilibrated with 1X PBS pH 7.6. Elution fractions corresponding to monomer (~30 kDa) were pooled and concentrated using Amicon Ultra Centrifugal Filters MWCO 10,000 (Millipore). The concentrated protein was filtered through a 0.22 μm filter before aliquoting for storage at -80 °C.

Polyacrylamide Gel Electrophoresis

Aliquots of protein samples collected at various purification steps were analyzed by 15% SDS-PAGE. Concentrated scFv was also analyzed by 6% Native-PAGE. Gels were stained using Coomassie-Blue Stain. After destaining with 40% methanol and 10% acetic acid, gel images were taken using the Fotodyne Imaging system (Fotodyne Inc.).

Circular Dichroism (CD) Spectroscopy

To confirm the secondary structure of refolded KD-247 scFv in comparison to KD-247 F_{ab}, we used far-UV CD, which measures the ellipticity (θ) of the protein sample from 200 to 240 nm wavelength. KD-247 F_{ab} and refolded scFv were diluted with 1X PBS to 200 μg/ml. 250 μl of each sample was analyzed at 25 °C or 37 °C using a 1 mm quartz cuvette in a J-815 CD Spectrometer (JASCO). For interaction with V3 peptide, 300 μl of 200 μg/ml sample was mixed with 6 μl of 1 mM V3 peptide (KRKRIHIGPGRAFYTT) derived from HIV-1 MN and incubated on ice overnight before analysis. Circular dichroism spectra were plotted using GraphPad Prism 5 (GraphPad Software Inc.).

NIH-PA Author Manuscript

NIH-PA Author Manuscript

NIH-PA Author Manuscript

Preparation of HIV-1 Virus and HIV-1 Env Pseudotyped Virus

pWT/BaL plasmid was obtained through the NIH AIDS Research and Reference Reagent Program (NIH ARRRP) from B.R. Cullen (Duke University). In a 75 cm^2 flask, 1.8×10^6 293T cells were transfected with 8 μg pWT/BaL using FuGENE 6 (Roche) in a 3:1 ratio. Supernatant containing virions was collected at 72 hours after transfection. After centrifugation at 1,100 rpm for 5 minutes at 4 °C, the supernatant was subsequently filtered through a 0.45 μm filter before storage at -80 °C. The same protocol was used for the production of HIV-1 Env pseudotyped virus. HIV-1 backbone plasmid with Env deletion, pSG3ΔEnv, was obtained through the NIH ARRRP from Drs. John C. Kappes and Xiaoyun Wu (University of Alabama at Birmingham). Plasmid for expression of JR-FL Env ($pEnv_{JR\text{-}FL}$) was provided by Dr. Shuzo Matsushita (Kumamoto University). Plasmid for ZM53M.PB12 Env ($pEnv_{ZM53M.PB12}$) was obtained through NIH ARRRP from Drs C.A. Derdeyn and E. Hunter (Emory University). 293T cells were co-transfected with 5.3 μg pSG3ΔEnv and 2.7 μg $pEnv_{JR\text{-}FL}$ (2:1 ratio). The amount of infectious virus in the supernatant was quantified using the $TCID_{50}$ assay as previously described (30).

TZM-bl Cell-Based Neutralization Assay

The ability of KD-247 scFv to neutralize HIV-1 virions was tested in a TZM-bl cell-based neutralization assay as previously described with some modifications (30). TZM-bl cells were obtained through the NIH ARRRP from Dr. John C. Kappes, Dr. Xiaoyun Wu and Tranzyme Inc. Maraviroc (obtained through NIH ARRRP), KD-247 F_{ab} and scFv were diluted to various concentrations in PBS. HIV-1 BaL virus or JR-FL Env pseudotyped virus (final: 50 $TCID_{50}$) was diluted in infection medium (DMEM, 10% FBS, 1X Penicillin/ Streptomycin, 20 μg/ml DEAE-Dextran). 50 μl of sample dilutions and virus or pseudotyped virus were pre-incubated at 37 °C for 1 hour prior to infection of TZM-bl cells (pre-seeded in 96-well plate with 100 μl of 1×10^4 cells per well). Luciferase activity of infected TZM-bl cells was determined at 48 hours post-infection using Bright-Glo Reagent (Promega) according to the manufacturer's instructions. Luminescence was measured using an EnSpire Plate Reader (Perkin Elmer). Neutralization assays were carried out at least two times with duplicates each time. The relative light unit (RLU) was adjusted based on luminescence reading of the cell control (non-infected cells). The mean RLU was used to calculate percent infection relative to the mean RLU of virus control (infected cells only). Percent infection was plotted as a function of sample concentration (in logarithmic scale) using GraphPad Prism 5 to determine 50% inhibitory or neutralizing concentration (IC_{50}).

RESULTS

Construction of KD-247 scFv

To better understand the molecular interaction of KD-247 with its epitope, $Isoleucine^{311}$-$Glycine^{312}$-$Proline^{313}$-$Glycine^{314}$-$Arginine^{315}$ (IGPGR), which is located at the tip of HIV-1 V3 loop, we have constructed KD-247 in the form of a single-chain variable fragment (scFv). The V_H and V_L of KD-247 scFv are linked with a 20 amino acid-long linker, which consists of four repeats of the Glycine-Glycine-Glycine-Glycine-Serine sequence (Fig. 1A), to enable expression of monomeric scFv (18). The gene of KD-247 scFv optimized for *E. coli* expression was subcloned into the pET28a3c vector (Fig. 1B) for the overexpression of scFv with an N-terminal 6X Histidine (HIS_6) tag (Fig. 1A). In addition to the thrombin cleavage site, pET28a3c contains a 3C protease cleavage site for cleavage of the HIS_6 tag when necessary (Fig. 1B).

NIH-PA Author Manuscript NIH-PA Author Manuscript NIH-PA Author Manuscript

Optimization of KD-247 scFv Expression

To purify KD-247 scFv using an *E. coli* expression system, our first attempt was to express KD-247 scFv in Origami 2 (DE3) pLysS, which was engineered for the cytoplasmic expression of the recombinant protein with proper protein folding. When the scFv was expressed and induced at 37 °C using various IPTG concentrations, a distinct protein band of size approximately 30 kDa could be identified in the pellet fractions of cell lysates with the exception of the non-induced cells (Fig. 2A). This observation indicated that the overexpression of KD-247 scFvs in the cytoplasm had resulted in the aggregation of improperly folded protein in a form commonly known as inclusion bodies. Despite many efforts of optimizing the expression of KD-247 scFv, including inducing at 30 °C (Fig. 2B) and expressing in different *E. coli* strains (Fig. 2C), KD-247 scFv remained insoluble.

Purification of KD-247 scFv from Inclusion Bodies

Although the overexpression of KD-247 scFv failed to yield soluble protein, we were able to establish a system to recover and purify KD-247 scFv from the inclusion bodies (Fig. 3). Briefly, inclusion bodies isolated from cell lysate after sonication were washed extensively to eliminate the majority of cellular debris before denaturation using 6 M guanidine-hydrochloride (Gu-HCl) in the presence of β-mercaptoethanol. Denatured scFv was dissolved using buffer containing 6 M urea. Next, dialysis of denatured scFv against buffer containing 0.8 M urea enabled gradual refolding of denatured scFv to partially folded intermediates with the assistance of a cysteine-cystine redox reagent to help with disulfide bond formation. Finally, partially folded intermediates were immobilized on a nickel column for gradient wash to remove excess denaturing reagent. SDS-PAGE shows that scFv of ~ 30 kDa can be detected in the pellet of cell lysate, supernatant of denaturation (Fig. 4A), and the elution from nickel column (Fig. 4B). The refolded scFvs consist of multiple folded species and can be separated using size-exclusion chromatography (Fig.4C). The monomeric scFv was collected and concentrated for downstream assays. On native-PAGE, the concentrated KD-247 scFv appeared as a distinct band and migrated faster than the KD-247 F_{ab}, confirming that its native form is a monomer.

Far-UV Circular Dichroism Spectroscopy

To confirm the proper folding of scFv into the immunoglobulin structure which consists primarily of β-sheets (1,18), we performed far-UV circular dichroism (CD) spectroscopy (19). CD spectra of refolded KD-247 scFv with and without V3 peptide are very similar to that of KD-247 F_{ab} (Figs. 5A &B). This indicates that the bacterially expressed KD-247 scFv can be refolded into a form that is comparable to KD-247 F_{ab}, which is obtained from a eukaryotic expression system. Furthermore, the β-sheet profiles of KD-247 scFv do not show significant differences when incubated at 37 °C for 1 hour and overnight (Fig. 5C).

Neutralization Assay

To further evaluate the biological activity of KD-247 scFv, we performed an HIV-1 neutralization assay using TZM-bl cells. As shown in Table 2, the refolded KD-247 scFv is able to neutralize clade B HIV-1 or pseudotyped HIV-1 (with GPGR V3 loop), but not clade C pseudotyped HIV-1 (with GPGQ V3 loop). KD-247 scFv neutralizes HIV-1 BaL and JR-FL Env pseudotyped HIV-1 with 50% neutralizing concentration (IC_{50}) comparable to the KD-247 F_{ab}. As expected, both KD-247 scFv and F_{ab} cannot neutralize ZM53M.PB12 (Clade C) Env pseudotyped HIV-1. Maraviroc, which targets the CCR5 coreceptor, is able to inhibit the entry of the HIV-1 and pseudotyped HIV-1 viruses examined in this assay.

NIH-PA Author Manuscript NIH-PA Author Manuscript NIH-PA Author Manuscript

DISCUSSION

In human adaptive immune system, B lymphocytes play the role of producing antibodies that are specific to a foreign antigen, such as virus, microbes and parasites (1). Human neutralizing antibody produced in nature are consist of a pair of identical heavy and light chains with three constant domains on the heavy chain and one constant domain on the light chain. Each variable domain on the heavy and light chains contains the complementarity determining regions (CDRs) that are responsible for the binding to the antigen (1,4,28). Innovative recombinant DNA technologies have made possible the modification of an antibody into smaller binding fragments such as scFv, in which the antigen binding sites can be retained (1,17,18,22,28,34). scFv format has been widely used in the phage display system because of its relatively small size to allow genetic engineering in the bacterial system (1,45,18,22,28,41). In this study, we have shown that KD-247 scFv, which was expressed in a bacterial system, can be successfully recovered from inclusion bodies through refolding. The refolded KD-247 scFv showed secondary structure and neutralizing activity comparable to KD-247 F_{ab}, which was obtained from the eukaryotic expression system.

To date, several refolding systems from insoluble scFv have been reported (15,26,39,42). Tsumoto K. and colleagues have described the use of glutathione and the addition of L-arginine in the refolding process of scFv (42). The on-column refolding approach based on the nickel-affinity chromatography has been described by other groups (15,26). Our system reported here is based on a combination of these protocols performed in a step-wise fashion with the addition of the redox reagents cysteine and cystine. The presence of disulfide bonds in the scFv can be a challenge in the proper expression of recombinant protein in the reducing environment of the *E. coli* cytoplasm (14). To address the issue of obtaining soluble scFv, we are still investigating the use of other protein expression vectors containing fusion tags that may help with the expression of soluble recombinant protein.

Using the purification protocol described here, we have purified KD-247 scFv from inclusion bodies and refolded the protein *in vitro* under the artificial control of cysteine and cystine to enable formation of intradomain disulfide bonds. The yield of purified, refolded scFv was comparably lower than the yield of soluble protein obtained from overexpression. This is possibly due to the loss of protein at each step of purification and during concentration. Although the yield is sufficient for subsequent assays such as far-UV CD and HIV-1 neutralization assay, optimization of this system will be needed to obtain sufficiently large quantity of protein for X-ray crystallography studies.

The refolded KD-247 scFv showed comparable neutralization profile compared to KD-247 F_{ab}. Their abilities to neutralize only clade B HIV-1 (GPGR V3 loop) but not clade C HIV-1 (GPGQ V3 loop), also further confirm the neutralization studies as previously described using KD-247 mAb (12,27). Using this system, we are currently engineering KD-247 scFv variants, which are designed based on our molecular modeling studies to alter the binding site of KD-247 and which we expect to exhibit improved neutralizing profiles in future studies.

Acknowledgments

We would like to thank Dr. Mark Palmier for suggestions on the optimization of the protein refolding protocol. We also acknowledge Dr. Krishna K. Sharma for use of the circular dichroism spectrometer. This work was supported in part by NIH grants AI076119, AI094715, AI074389 and from the Ministry of Knowledge and Economy, Bilateral International Collaborative R&D Program, Republic of Korea (S.G.S.). L.A.C. is supported by the MU-HHMI C3 Program. B.M. is a recipient of the amfAR Mathilde Krim Fellowship and a Canadian Institutes of Health Research (CIHR) Fellowship.

NIH-PA Author Manuscript NIH-PA Author Manuscript NIH-PA Author Manuscript

ABBREVIATIONS

θ	ellipticity
ARRRP	AIDS Research and Reference Reagent Program
CCR5	C-C chemokine receptor type 5
CD	circular dichroism
CD4	cluster of differentiation 4
CDR	complementarity determining region
CXCR-4	C-X-C chemokine receptor type 4
DMEM	Dulbecco's Modified Eagle's Medium
E. coli	Escherichia coli
Env	envelope glycoprotein
F_{ab}	antigen binding fragment
FBS	fetal bovine serum
FDA	Food and Drug Administration
gp120	glycoprotein 120
gp41	glycoprotein 41
GPGR	$Glycine^{312}$-$Proline^{313}$-$Glycine^{314}$-$Arginine^{315}$
GPGQ	$Glycine^{312}$-$Proline^{313}$-$Glycine^{314}$-$Arginine^{315}$
Gu-HCl	guanidine-hydrochloride
HAART	Highly Active Anti-Retroviral Therapy
HIS_6	6x-histidine tag
HIV-1	Human Immunodeficiency Virus Type 1
IC_{50}	50% inhibitory or neutralizing concentration
IGPGR	Isoleucine-Glycine-Proline-Glycine-Arginine
IPTG	isopropyl-β-D-thiogalactopyranoside
LB	Luria-Bertani broth
mAb	monoclonal antibody
MWCO	molecular weight cut-off
NIH	National Institutes of Health
OD_{600nm}	optical density at 600 nm
PAGE	polyacrylamide gel electrophoresis
PBS	phosphate buffered saline
PMSF	phenylmethylsulfonyl fluoride
RLU	relative light unit
rpm	revolutions per minute
scFv	single-chain variable fragments

NIH-PA Author Manuscript NIH-PA Author Manuscript NIH-PA Author Manuscript

SDS	sodium dodecyl sulfate
$TCID_{50}$	50% tissue culture infectious dose
UV	ultraviolet
V3	third hypervariable
V_H	heavy chain variable domain
V_L	light chain variable domain

REFERENCES

1. Abbas, AK.; Lichtman, AH. Cellular and Molecular Immunology. 5th ed. Elsevier Saunders; Pennsylvania, USA: 2005. Antibodies and Antigens.; p. 43-79.
2. Balazs AB, Chen J, Hong CM, Rao DS, Yang L, Baltimore D. Antibody-based protection against HIV infection by vectored immunoprophylaxis. Nature. 2012; 481:81–84. [PubMed: 22139420]
3. Barbas CF 3rd, Hu D, Dunlop N, Sawyer L, Cababa D, Hendry RM, Nara PL, Burton DR. In vitro evolution of a neutralizing human antibody to human immunodeficiency virus type 1 to enhance affinity and broaden strain cross-reactivity. Proc. Natl. Acad. Sci. U. S. A. 1994; 91:3809–3813. [PubMed: 8170992]
4. Burton, DR. Antibody Libraries.. In: Barbas, CF.; Burton, DR.; Scott, JK.; Silverman, GJ., editors. Phage Display, A Laboratory Manual. Cold Spring Harbor Laboratory Press; New York: 2000. p. 3.1-3.18.
5. Chen W, Dimitrov DS. Human monoclonal antibodies and engineered antibody domains as HIV-1 entry inhibitors. Curr. Opin. HIV AIDS. 2009; 4:112–117. [PubMed: 19339949]
6. Dalgleish AG, Beverley PC, Clapham PR, Crawford DH, Greaves MF, Weiss RA. The CD4 (T4) antigen is an essential component of the receptor for the AIDS retrovirus. Nature. 1984; 312:763–767. [PubMed: 6096719]
7. De Clercq E. Anti-HIV drugs: 25 compounds approved within 25 years after the discovery of HIV. Int. J. Antimicrob. Agents. 2009; 33:307–320. [PubMed: 19108994]
8. DeLano, WL. The PyMOL Molecular Graphics System. DeLano Scientific; Palo Alto, CA, USA: 2002. http://www.pymol.org
9. Doms RW. Chemokine receptors and HIV entry. AIDS. 2001; 15(Suppl 1):S34–35. [PubMed: 11403007]
10. Doms RW, Moore JP. HIV-1 membrane fusion: targets of opportunity. J. Cell Biol. 2000; 151:F9–14. [PubMed: 11038194]
11. Dorr P, Westby M, Dobbs S, Griffin P, Irvine B, Macartney M, Mori J, Rickett G, Smith-Burchnell C, Napier C, Webster R, Armour D, Price D, Stammen B, Wood A, Perros M. Maraviroc (UK-427,857), a potent, orally bioavailable, and selective small-molecule inhibitor of chemokine receptor CCR5 with broad-spectrum anti-human immunodeficiency virus type 1 activity. Antimicrob. Agents Chemother. 2005; 49:4721–4732. [PubMed: 16251317]
12. Eda Y, Takizawa M, Murakami T, Maeda H, Kimachi K, Yonemura H, Koyanagi S, Shiosaki K, Higuchi H, Makizumi K, Nakashima T, Osatomi K, Tokiyoshi S, Matsushita S, Yamamoto N, Honda M. Sequential immunization with V3 peptides from primary human immunodeficiency virus type 1 produces cross-neutralizing antibodies against primary isolates with a matching narrow-neutralization sequence motif. J. Virol. 2006; 80:5552–5562. [PubMed: 16699036]
13. Frigerio B, Canevari S, Figini M. Antibody engineering as opportunity for selection and optimization of anti-HIV therapeutic agents. The Open Autoimmunity Journal. 2010; 2:127–138.
14. Guglielmi L, Martineau P. Expression of single-chain Fv fragments in E. coli cytoplasm. Methods Mol. Biol. 2009; 562:215–224. [PubMed: 19554299]
15. Guo JQ, Li QM, Zhou JY, Zhang GP, Yang YY, Xing GX, Zhao D, You SY, Zhang CY. Efficient recovery of the functional IP10-scFv fusion protein from inclusion bodies with an on-column refolding system. Protein Expr. Purif. 2006; 45:168–174. [PubMed: 16125970]

NIH-PA Author Manuscript NIH-PA Author Manuscript NIH-PA Author Manuscript

16. Hessell AJ, Haigwood NL. Neutralizing antibodies and control of HIV: moves and countermoves. Curr. HIV/AIDS Rep. 2011
17. Holliger P, Hudson PJ. Engineered antibody fragments and the rise of single domains. Nat Biotechnol. 2005; 23:1126–1136. [PubMed: 16151406]
18. Huston JS, Mudgett-Hunter M, Tai MS, McCartney J, Warren F, Haber E, Oppermann H. Protein engineering of single-chain Fv analogs and fusion proteins. Methods Enzymol. 1991; 203:46–88. [PubMed: 1762568]
19. Kelly SM, Jess TJ, Price NC. How to study proteins by circular dichroism. Biochim. Biophys. Acta. 2005; 1751:119–139. [PubMed: 16027053]
20. Kipriyanov SM. High-level periplasmic expression and purification of scFvs. Methods Mol. Biol. 2009; 562:205–214. [PubMed: 19554298]
21. Klatzmann D, Champagne E, Chamaret S, Gruest J, Guetard D, Hercend T, Gluckman JC, Montagnier L. T-lymphocyte T4 molecule behaves as the receptor for human retrovirus LAV. Nature. 1984; 312:767–768. [PubMed: 6083454]
22. Kontermann RE. Alternative antibody formats. Curr. Opin. Mol. Ther. 2010; 12:176–183. [PubMed: 20373261]
23. Kwong PD, Mascola JR, Nabel GJ. Rational design of vaccines to elicit broadly neutralizing antibodies to HIV-1. Cold Spring Harb. Perspect. Med. 2011; 1:a007278. [PubMed: 22229123]
24. Kwong PD, Wyatt R, Robinson J, Sweet RW, Sodroski J, Hendrickson WA. Structure of an HIV gp120 envelope glycoprotein in complex with the CD4 receptor and a neutralizing human antibody. Nature. 1998; 393:648–659. [PubMed: 9641677]
25. Lalezari JP, Eron JJ, Carlson M, Cohen C, DeJesus E, Arduino RC, Gallant JE, Volberding P, Murphy RL, Valentine F, Nelson EL, Sista PR, Dusek A, Kilby JM. A phase II clinical study of the long-term safety and antiviral activity of enfuvirtide-based antiretroviral therapy. AIDS. 2003; 17:691–698. [PubMed: 12646792]
26. Liu M, Wang X, Yin C, Zhang Z, Lin Q, Zhen Y, Huang H. One-step on-column purification and refolding of a single-chain variable fragment (scFv) antibody against tumour necrosis factor alpha. Biotechnol. Appl. Biochem. 2006; 43:137–145. [PubMed: 16293104]
27. Matsushita S, Takahama S, Shibata J, Kimura T, Shiozaki K, Eda Y, Koito A, Murakami T, Yoshimura K. Ex vivo neutralization of HIV-1 quasi-species by a broadly reactive humanized monoclonal antibody KD-247. Hum. antibodies. 2005; 14:81–88. [PubMed: 16720978]
28. Maynard J, Georgiou G. Antibody engineering. Annu. Rev. Biomed. Eng. 2000; 2:339–376. [PubMed: 11701516]
29. Melikyan GB. Common principles and intermediates of viral protein-mediated fusion: the HIV-1 paradigm. Retrovirol. 2008; 5:111.
30. Montefiori, DC. Measuring HIV Neutralization in a Luciferase Reporter Gene Assay.. In: Prasad, VR.; Kalpana, GV., editors. HIV Protocols. 2nd ed. Humana Press; New York: 2009. p. 395-415.
31. Ng CT, Jaworski JP, Jayaraman P, Sutton WF, Delio P, Kuller L, Anderson D, Landucci G, Richardson BA, Burton DR, Forthal DN, Haigwood NL. Passive neutralizing antibody controls SHIV viremia and enhances B cell responses in infant macaques. Nat. Med. 2010; 16:1117–1119. [PubMed: 20890292]
32. Parren PW, Burton DR, Sattentau QJ. HIV-1 antibody--debris or virion? Nat. Med. 1997; 3:366–367. [PubMed: 9095159]
33. Progress report 2011: Global HIV/AIDS Response. WHO; UNAIDS; UNICEF; 2012. http://www.who.int/hiv/pub/progress_report2011/en/index.html
34. Rader, CB.; Barbas, CF, 3rd. Antibody Engineering.. In: Barbas, CF.; Burton, DR.; Scott, JK.; Silverman, GJ., editors. Phage Display, A Laboratory Manual. Cold Spring Harbor Laboratory Press; New York: 2000. p. 13.1-13.15.
35. Rizzuto C, Sodroski J. Fine definition of a conserved CCR5-binding region on the human immunodeficiency virus type 1 glycoprotein 120. AIDS Res. Hum. Retroviruses. 2000; 16:741–749. [PubMed: 10826481]
36. Rizzuto CD, Wyatt R, Hernandez-Ramos N, Sun Y, Kwong PD, Hendrickson WA, Sodroski J. A conserved HIV gp120 glycoprotein structure involved in chemokine receptor binding. Science. 1998; 280:1949–1953. [PubMed: 9632396]

NIH-PA Author Manuscript NIH-PA Author Manuscript NIH-PA Author Manuscript

37. Rucker J, Samson M, Doranz BJ, Libert F, Berson JF, Yi Y, Smyth RJ, Collman RG, Broder CC, Vassart G, Doms RW, Parmentier M. Regions in beta-chemokine receptors CCR5 and CCR2b that determine HIV-1 cofactor specificity. Cell. 1996; 87:437–446. [PubMed: 8898197]
38. Sattentau QJ, Moore JP. Conformational changes induced in the human immunodeficiency virus envelope glycoprotein by soluble CD4 binding. J. Exp. Med. 1991; 174:407–415. [PubMed: 1713252]
39. Sinacola JR, Robinson AS. Rapid refolding and polishing of single-chain antibodies from Escherichia coli inclusion bodies. Protein Expr. Purif. 2002; 26:301–308. [PubMed: 12406685]
40. Thali M, Moore JP, Furman C, Charles M, Ho DD, Robinson J, Sodroski J. Characterization of conserved human immunodeficiency virus type 1 gp120 neutralization epitopes exposed upon gp120-CD4 binding. J. Virol. 1993; 67:3978–3988. [PubMed: 7685405]
41. Thie H, Voedisch B, Dubel S, Hust M, Schirrmann T. Affinity maturation by phage display. Methods Mol. Biol. 2009; 525:309–322. [PubMed: 19252854]
42. Tsumoto K, Shinoki K, Kondo H, Uchikawa M, Juji T, Kumagai I. Highly efficient recovery of functional single-chain Fv fragments from inclusion bodies overexpressed in Escherichia coli by controlled introduction of oxidizing reagent--application to a human single-chain Fv fragment. J. Immunol. Methods. 1998; 219:119–129. [PubMed: 9831393]
43. Wei X, Decker JM, Wang S, Hui H, Kappes JC, Wu X, Salazar-Gonzalez JF, Salazar MG, Kilby JM, Saag MS, Komarova NL, Nowak MA, Hahn BH, Kwong PD, Shaw GM. Antibody neutralization and escape by HIV-1. Nature. 2003; 422:307–312. [PubMed: 12646921]
44. Weissenhorn W, Hinz A, Gaudin Y. Virus membrane fusion. FEBS letters. 2007; 581:2150–2155. [PubMed: 17320081]
45. West AP Jr. Galimidi RP, Gnanapragasam PN, Bjorkman PJ. Single-chain Fv-based anti-HIV proteins: potential and limitations. J.Virol. 2012; 86:195–202. [PubMed: 22013046]
46. White JM, Delos SE, Brecher M, Schornberg K. Structures and mechanisms of viral membrane fusion proteins: multiple variations on a common theme. Crit. Rev. Biochem. Mol. Biol. 2008; 43:189–219. [PubMed: 18568847]
47. Wu L, Gerard NP, Wyatt R, Choe H, Parolin C, Ruffing N, Borsetti A, Cardoso AA, Desjardin E, Newman W, Gerard C, Sodroski J. CD4-induced interaction of primary HIV-1 gp120 glycoproteins with the chemokine receptor CCR-5. Nature. 1996; 384:179–183. [PubMed: 8906795]

NIH-PA Author Manuscript NIH-PA Author Manuscript NIH-PA Author Manuscript

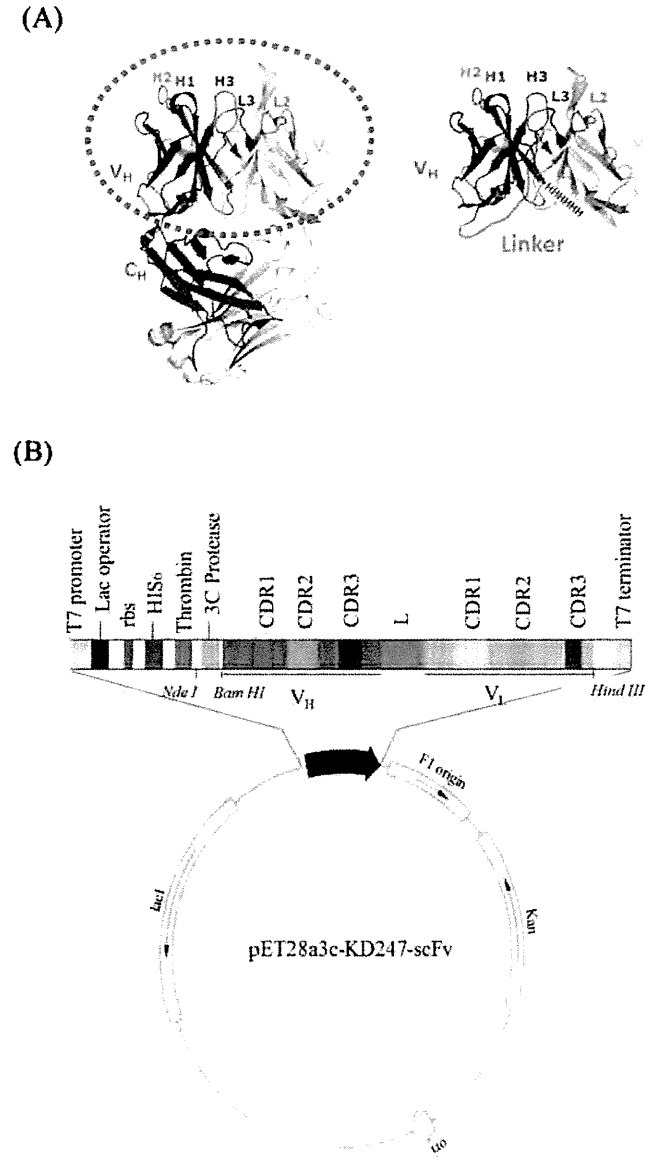

Figure 1.

Schematic diagram of pET28a3c-KD247-scFv. (A) The crystal structure of KD-247 F_{ab} (1.5 Å resolution, PDB: 3NTC) is shown with the complementarity determining regions (CDRs) highlighted in different colors. [Red: CDR 1 heavy chain (H1); Orange: CDR 2 heavy chain (H2); Purple: CDR 3 heavy chain (H3); Yellow: CDR 1 light chain (L1); Green: CDR 2 light chain (L2); Dark blue: CDR3 light chain (L3)]. The expected structure of KD-247 scFv was illustrated as a model. Figures were generated using PyMOL (8). (B) The variable domains of the heavy chain (V_H) and light chain (V_L) of KD-247 are connected with a peptide linker (L) to form the scFv. The twenty amino acid long peptide linker consists of four repeats of Glycine-Glycine-Glycine-Glycine-Serine, $(GGGGS)_4$. The scFv construct was subcloned at the N-terminal 6X Histidine tag (HIS_6) of the pET28a3c vector.

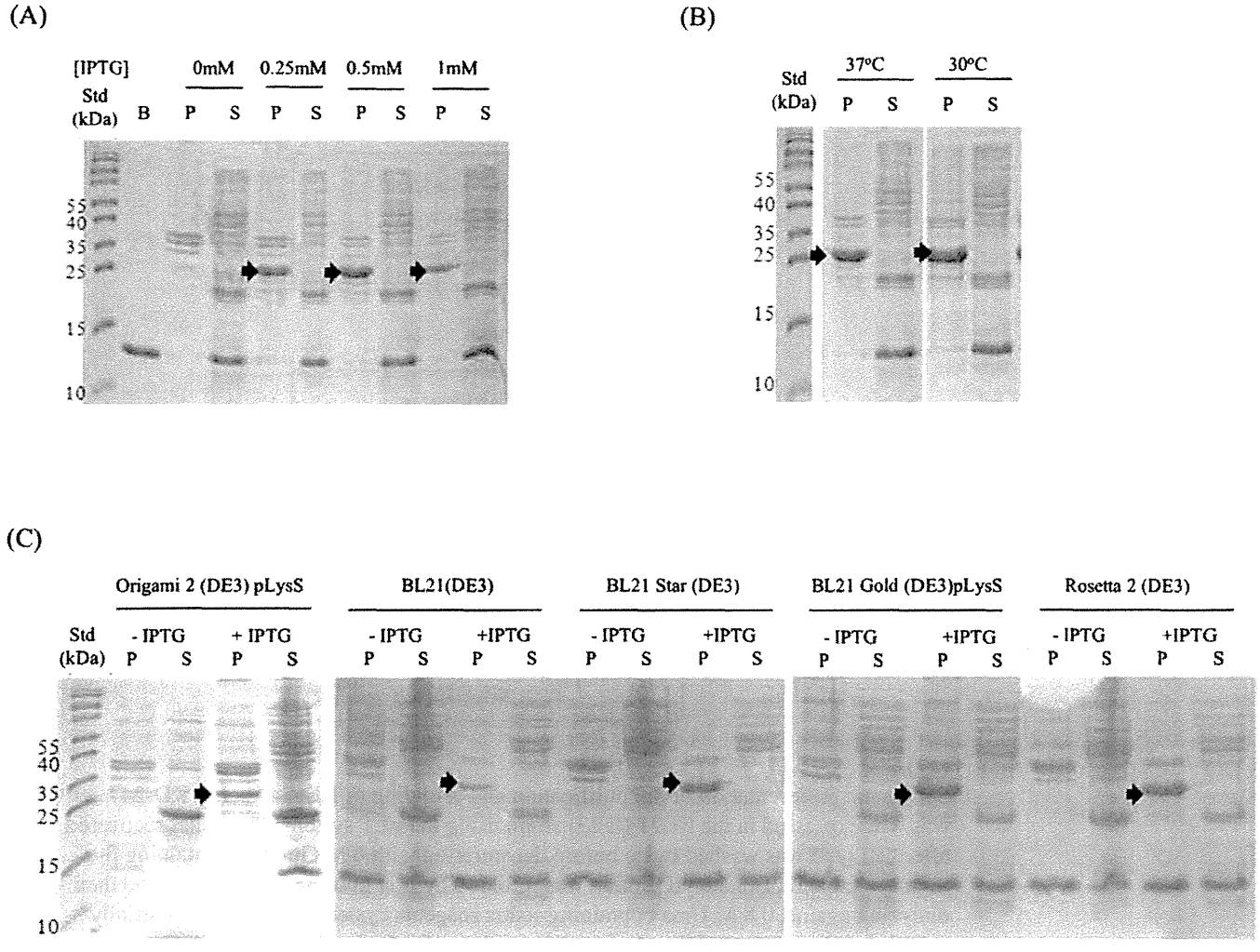

Figure 2.

SDS-PAGE showing the optimization of KD-247 scFv overexpression in *E. coli*. (A) Overexpression of KD-247 scFv in Origami 2 (DE3) pLysS at various IPTG concentrations (0.25 mM, 0.5 mM, and 1 mM) were examined. (B) KD-247 scFv expression was induced at 37 °C or 30 °C. (C) Overexpression of KD-247 scFv in various *E. coli* strains was compared. As shown by the arrows, KD-247 scFv was expressed as inclusion bodies in *E. coli*. [Std: Protein standards; P: Pellet; S: Supernatant; B: Lysis Buffer]

NIH PA Author Manuscript NIH PA Author Manuscript NIH PA Author Manuscript